$^{31}P(^3He,d)^{32}S$ reaction at 25 MeV

J. Kalifa, J. Vernotte, Y. Deschamps, F. Pougheon, G. Rotbard, and M. Vergnes
Institut de Physique Nucléaire, BP 1, 91406 Orsay, France

B. H. Wildenthal*
Institut de Physique Nucléaire, BP 1, 91406 Orsay, France
and Cyclotron Laboratory† Michigan State University, East Lansing, Michigan 48824
(Received 27 December 1977)

The $^{31}P(^3He,d)$ ^{32}S reaction was investigated at 25 MeV incident energy. One-hundred and eleven levels up to an excitation energy of 12.5 MeV were observed using a split-pole magnetic spectrograph. The experimental angular distributions were analyzed with the distorted-wave Born approximation. The optical model parameters used in the distorted-wave Born-approximation calculations were obtained from a fit to elastic ^3He scattering data taken on ^{31}P at 25 MeV. Gamow functions were used as form factors for the transferred proton in the case of unbound states. Values of the transferred orbital angular momenta l and spectroscopic strengths were obtained for sixty levels, with many odd-parity levels being observed above 9 MeV excitation. Spin and parity assignments were made upon the basis of the l values obtained from the shapes of the angular distributions and upon comparison with the results of other reactions. Isospin assignments were made by comparison with ^{32}P levels. Except for the $l_p = 1$, $T = 0$ transfers, most of the observed spectroscopic strength is concentrated into a few levels. The existence of a T-mixed doublet of levels, $J^\pi = 1^-$, is suggested in the 11 MeV region of excitation. The excitation energies and spectroscopic strengths are compared with results of a recent shell-model calculation.

[NUCLEAR REACTIONS $^{31}P(^3He,d)$, $^{31}P(^3He,{}^3He)$, $E=25$ MeV; measured $\sigma(E_d,\theta)$, ^{32}S deduced levels, l, J, π, T, spectroscopic strengths; measured $\sigma(\theta)$, deduced optical model parameters. DWBA analysis using Gamow functions as form factors.]

I. INTRODUCTION

The most extensive study of the nucleus ^{32}S through the $^{31}P(^3He,d)^{32}S$ reaction was done some years ago at 12 MeV by Graue *et al.*[1] In this study levels were observed up to 9.5 MeV. According to the sum rules of MacFarlane and French[2] most of the $l=0$ and 2 stripping strengths were observed, but a large part of the $l=1$ and 3 strengths was missing and is expected to lie at higher excitation energies. The first aim of the present work is to extend the knowledge of the $^{31}P(^3He,d)$ ^{32}S reaction to levels above 9.5 MeV, and especially to look for the $l=1$ and 3 strength which is carried by the few levels ($E_x=10.0$–10.4 MeV, $J^\pi=2^-$, 3^-, and 4^-, $T=1$) strongly populated in the $^{31}P(p,\gamma)^{32}S$ reaction.[3] Towards this aim levels in ^{32}S were observed up to an excitation energy of 12.5 MeV and the angular distributions obtained were analyzed with the distorted-wave Born approximation (DWBA). Special attention was given to proton-unbound levels above $E_x=8864$ keV. It was possible to identify some of the currently observed stripping levels with resonance levels previously observed in proton or/and α-capture reactions. Isospin assignments to some ^{32}S levels were made by comparison with spectroscopic information from the $^{31}P(d,p)^{32}P$ reaction.[4]

Using the comprehensive set of spectroscopic factors and energies obtained in the present work, augmented by the results of previous proton stripping[1,5] studies and by results of recent pickup experiments,[6,7] the second aim of the present study is to evaluate the present understanding of the nuclear structure of ^{32}S as it is specifically revealed in the single-nucleon stripping process. To this end, the experimental results are discussed in terms of sum rules and in comparison to a new shell-model calculation for the positive-parity levels of ^{32}S.

II. EXPERIMENTAL PROCEDURES

A 25 MeV ^3He beam from the Orsay MP tandem Van de Graaff accelerator was used for the present experiment. The targets (60–120 $\mu g/cm^2$) were prepared by evaporation in vacuum of red phosphorus[8] on carbon backings about 15 $\mu g/cm^2$ thick. A surface barrier detector mounted inside the scattering chamber at $\theta_{lab}=53°$ with respect to the beam direction was used as a monitor during the angular distribution measurements.

Deuterons were momentum analyzed with an Enge split-pole magnetic spectrograph and were

detected by an array of six position-sensitive solid-state detectors (PSD). These were 50 mm long, 10 mm high, and either 650 or 1000 μm thick. The energy-loss signal from each detector was used to identify the particles. The signals from all events in the PSD were stored on a magnetic tape after processing by a T1600 Télémécanique computer. The division of the position signal by the deuteron energy-loss signal was done on-line by the computer and the resulting deuteron spectra were displayed on an 8096-channel analyzer, which made live control of the experiment possible.

The spectrograph horizontal entrance aperture was set to 3° ($\Omega = 1.7$ msr) for the (^{3}He, d) reaction and to 1° for the elastic scattering measurements. In order to prevent the deterioration of the phosphorus targets, the beam intensity was restricted to about 500 nA of $^3He^{++}$. The overall resolution was about 18 keV full width at half maximum (FWHM) with the 60 μg/cm^2 target.

III. ENERGY-LEVEL SPECTRA

Angular distribution data were taken at 16 angles ($5° \leq \theta_{lab} \leq 60°$) for the (^{3}He, d) reaction and at 31 angles ($9° \leq \theta_{lab} \leq 90°$) for the elastic scattering. A particle spectrum obtained at $\theta_{lab} = 10°$ with a target 120 μg/cm^2 thick is displayed on Fig. 1. Peaks due to the (^{3}He, d) reaction on ^{14}N and ^{16}O contaminants and ^{12}C and ^{13}C (carbon backing) are present in the spectra. The wide intense peak which results from deuterons feeding the ^{13}N levels at 3509 and 3547 keV prevented the observation of many ^{32}S levels between 11 and 12 MeV at more than three or four angles.

Reaction spectra were analyzed with the computer code AUTOFIT[9] to obtain peak positions

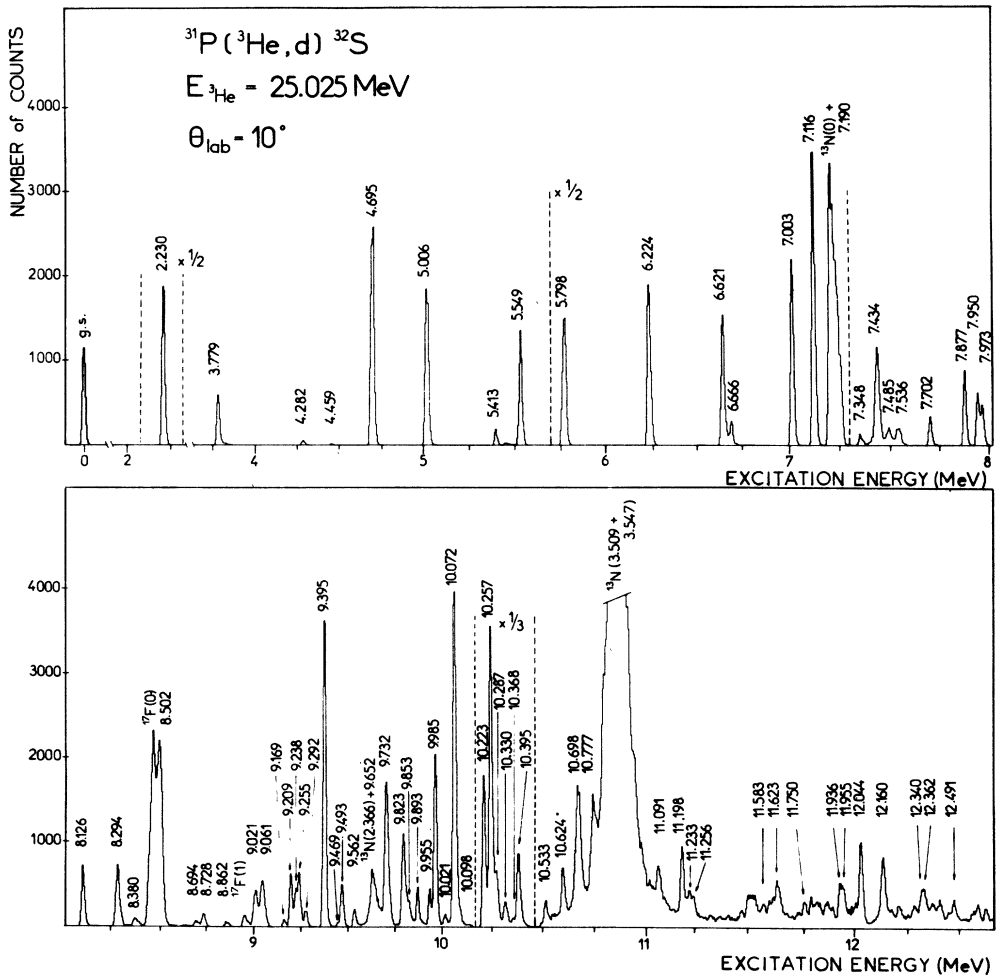

FIG. 1. Spectrum of the ^{31}P(^{3}He, d)^{32}S reaction at $\theta_{lab} = 10°$ obtained with an array of six position sensitive detectors. Because dead zones exist between the detectors this spectrum is constructed of three overlapping spectra.

and integrated counts in the individual peaks. Excitation energies were obtained from the peak positions using a two-step procedure. In the first step a relationship between the radius of curvature ρ of a particle in the spectrograph and the relevant position on a PSD (obtained using 8.78 MeV α particles from a ThC source) was used to get the excitation energies for all the peaks observed at the various angles. In the second step a small linear correction (from -5 keV at $E_x \simeq 5$ MeV to -20 keV at $E_x \simeq 12$ MeV) was made to these energies using accurately known values of some of the excitation energies.[3,10,11] The total accuracy is estimated to be ±5 keV for the $E_x \leq 9$ MeV levels and ±10 keV for the other ones.

Several levels observed in proton radiative capture experiments[11] are separated from each other by less than the 18 keV energy resolution available in the present experiment. Hence if they are populated in the stripping reaction they will appear as a single peak in the deuteron spectra. Special attention was therefore given to the analysis of the corresponding angular distributions. Furthermore, above 11.2 MeV, due to the difficulty of clearly defining the background and a standard peak shape, the number of counts extracted by the AUTOFIT code can be somewhat uncertain: In this energy range the angular distribution measurements were analyzed only for some strongly excited (and apparently corresponding to a single level) peaks.

Absolute cross sections to within ±15% were obtained by normalization to the 25 MeV ^{3}He scattering data at $\theta_{lab} = 9°$. At angles less than ~15°, the cross sections of ^{3}He elastic scattering on ^{31}P predicted by optical-model calculations are essentially invariant to details of the chosen optical-model parameters and the elastic-scattering data were assumed to have a cross-section normalization consistent with such predictions (76% of the Rutherford elastic-scattering cross section at $\theta_{lab} = 9°$).

IV. ANALYSIS OF ANGULAR DISTRIBUTIONS

The experimentally measured angular distributions were analyzed with the results of DWBA calculations using the relation

$$\left(\frac{d\sigma(\theta)}{d\omega}\right)_{exp} = 4.43 G_{l_j} \left(\frac{d\sigma_{l_j}(\theta)}{d\omega}\right)_{DWBA},$$

where 4.43 is the commonly used normalization factor for the (^{3}He, d) reaction[12] and $G_{l_j} = (2J_f+1)(2J_i+1)^{-1} C^2 S_{l_j}$ is the spectroscopic strength. J_i and J_f are the spins of the target and residual nuclei, respectively, and S_{l_j} is the spectroscopic factor. The isospin Clebsch-Gordan coefficient C^2 is equal to 0.5 for $T=0$ and $T=1$ states with $T_z = 0$.

DWBA cross sections were calculated with the computer code VENUS[13] for bound and proton-unbound states. Finite-range and nonlocality corrections were not included. Optical-model potentials used for all of these calculations are presented in Table I. The ^{3}He optical parameters were obtained from a fit to the present elastic-scattering data on ^{31}P using the computer code JIB3 .[14] Potentials of standard Woods-Saxon geometry with volume absorption were used. No spin-orbit term was included. Various starting optical-parameter sets were tried[15,16] and led to three sets ($V_R \simeq 80$, 140, and 180 MeV) which yielded similar fits to the elastic-scattering data. The set with $V_R \simeq 180$ MeV was adopted because it yields the best fit to the reaction data in the entire angular range for some strongly excited states (ground state, $l=0$; $E_x = 5798$ keV, $l=1$; $E_x = 2230$ keV, $l=2$; $E_x = 5006$ keV, $l=3$). The fit to the elastic-scattering data obtained with the $V_R = 180$ MeV set is shown in Fig. 2.

Various deuteron optical-parameter sets were tried for the analysis; a set adjusted for the ^{32}S case from average potentials derived by Newman *et al.*[17] was finally adopted. The proton bound-state potential is of the usual Woods-Saxon type

TABLE I. Optical-model parameters used in DWBA calculations.

Channel	E_{lab} (MeV)	V (MeV)	r (fm)	a (fm)	W (MeV)	r_W (fm)	a_W (fm)	$4W_D$ (MeV)	r (fm)	a (fm)	V_{so} (MeV)	r (fm)	a (fm)	r_c (fm)
^{31}P + ^{3}He	25	179.5	1.174	0.682	18.2	1.616	0.828							1.4
^{32}S + d	34.4	94.7	1.06	0.814				45.2	1.342	0.741	7	1.06	0.814	1.3
Proton bound state		a	1.25	0.65							6.25	1.25	0.65	1.25
Proton unbound state		b	1.25	0.65							6.25	1.25	0.65	1.25

[a] Adjusted by the computer code VENUS.
[b] Adjusted using the computer code GAMOV.

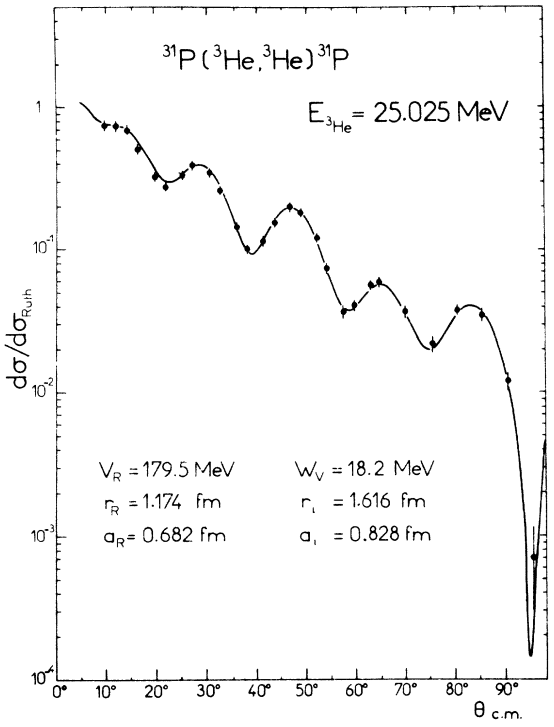

FIG. 2. Angular distribution of the elastic scattering of ^{3}He at 25 MeV on ^{31}P. Solid line is the optical model fit with the presented set of parameters.

with a well depth adjusted to reproduce the experimental proton separation energy.

Above $E_x > 8864$ keV states are proton unbound and a special treatment is needed to extract spectroscopic factors from the measured angular distributions. A DWBA analysis was done following the method developed by Coker *et al.*[18,19] In order to take into account the unbound nature of these levels the proton form factors were calculated using complex energy resonance eigenstates or Gamow functions $\tilde{g}_{l_j}(r)$ which are solutions of the radial Schrödinger equation for partial wave l_j for the system proton + target of reduced mass μ:

$$\left[-\frac{\hbar^2}{2\mu}\left(\frac{d^2}{dr^2}-\frac{l(l+1)}{r^2}\right)-\tilde{E}+U+U_{l_j}+U_c\right]\tilde{g}_{l_j}(r)=0\,,$$

where $\tilde{E}=E-\frac{1}{2}i\Gamma_{s.p.}$ is the complex c.m. energy of the system proton + target, and U, U_{l_j}, and U_c are the usual optical, spin-orbit, and Coulomb potentials, respectively. Numerical computation of $\tilde{g}_{l_j}(r)$ was performed using the GAMOV code[19] which, for a given optical potential, finds the complex energy $\tilde{E}$ at which the single-particle wave function asymptotically approaches a purely outgoing Coulomb wave of complex argument. In addition the single-particle width $\Gamma_{s.p.}=-2\,\mathrm{Im}\tilde{E}$ is obtained for each resonance level. This procedure appears to produce meaningful results since the proton partial widths Γ_p derived from the relation $\Gamma_p=C^2S_{l_j}\Gamma_{s.p.}$ are in good agreement for most of the levels presented in Table II with the Γ_p measured in proton elastic-scattering experiments.[3,10]

The DWBA analysis of transitions to levels of ^{32}S is straightforward when the J^π value of the level is known from other sources.[3,11,20-22] Since the ^{31}P target ground state is $\frac{1}{2}^+$, natural parity ^{32}S levels are populated by only one l transfer whereas mixed l and $l+2$ transfers can be involved in the population of unnatural-parity states. In

TABLE II. A comparison between the partial proton widths obtained through the relation $\Gamma_p=C^2S_p\Gamma_{s.p.}$ and through a proton elastic-scattering experiment (Ref. 3).

E_x (keV)	J^π	nl_j	V_p (MeV)	$\Gamma_{s.p.}$ (keV)	C^2S_p [a]	Γ_p (eV) [b]	Γ_p (eV) [c]
10072	2^-	$2p_{3/2}$	58.54	9.49	0.176	1670 ± 350	1600 ± 240
10223	3^-	$1f_{7/2}$	55.11	0.097	0.200	19 ± 4	16 ± 6
10257	4^-	$1f_{7/2}$	55.04	0.117	0.289	34 ± 7	45 ± 20
10287	3^-	$1f_{7/2}$	54.98	0.139	0.074	10 ± 2	9 ± 4
10330	1^-	$2p_{3/2}$	57.76	33.3	0.113	3760 ± 750	3800 ± 600
10368	2^+	$1d_{3/2}$	43.25	2.66	0.024	64 ± 13	30 ± 10
10395	4^-	$1f_{7/2}$	54.76	0.234	0.080	19 ± 4	25^{+20}_{-10}
12044	4^-	$1f_{7/2}$	51.34	23	0.031	710 ± 150	380 ± 70

[a] From the G_l values of the present work (Table III).
[b] From the relation $\Gamma_p=C^2S_p\Gamma_{s.p.}$ and assuming an accuracy of 20% for the spectroscopic factors.
[c] Reference 3.

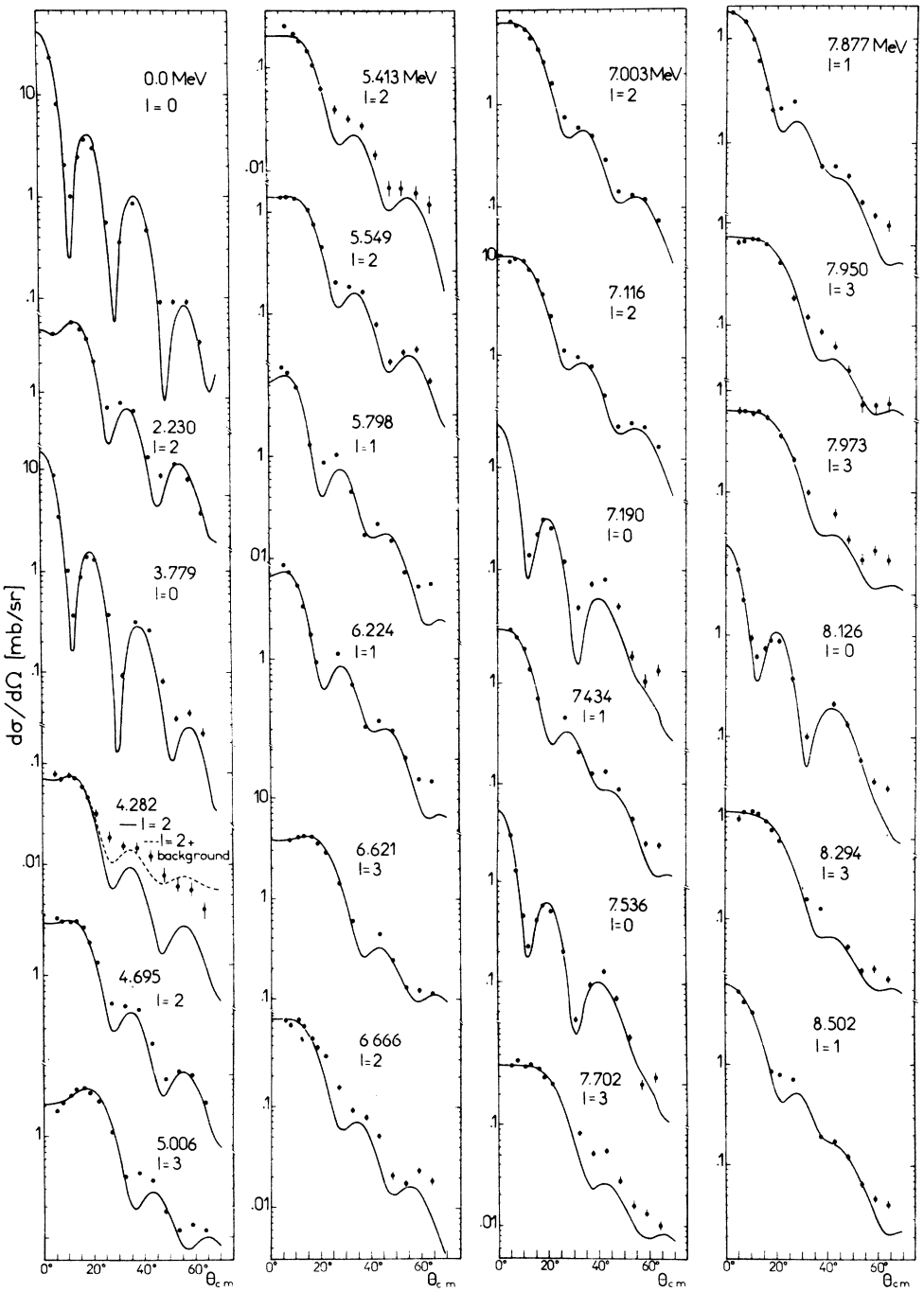

FIG. 3. Angular distributions of the $^{31}P(^{3}He,d)^{32}S$ reaction leading to proton-bound states. If not shown the error is less than the point size. Curves are DWBA predictions for the indicated l values.

these cases the amount of admixture of different l transfers was searched for by fitting the angular distributions by a superposition of the relevant theoretical curves. Up to an excitation energy of 10 MeV, 15% $l=2$ and less than 10% $l=0$ admixtures in predominantly $l=0$ and $l=2$ transfers, respectively, would result in a significantly different shape of the theoretical angular distributions. For the odd-parity states the amount of detectable l mixing depends slightly upon the excitation energy: A significant change of shape would be apparent with 35% $l=3$ and 5% $l=1$ ad-

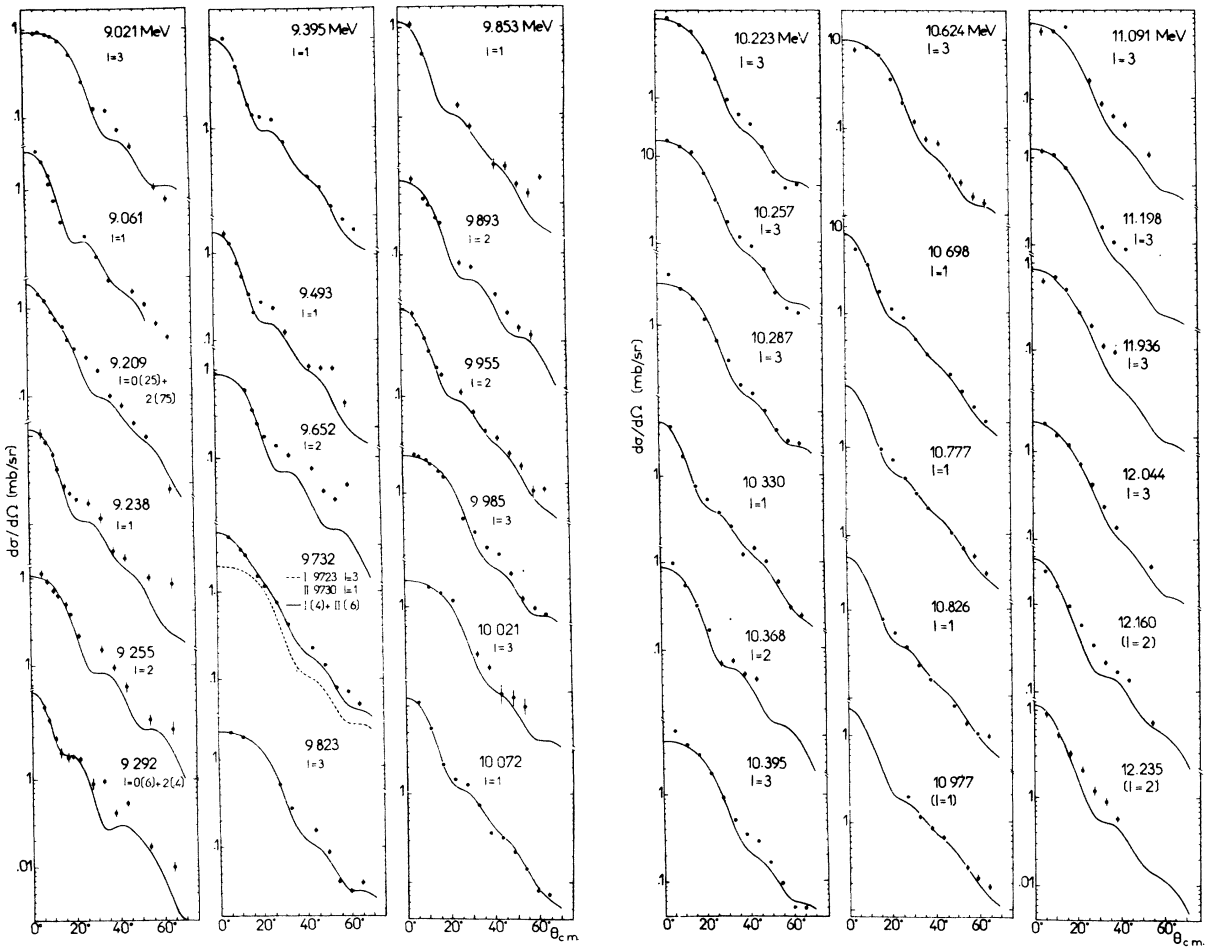

FIG. 4. Angular distributions of the $^{31}P(^3He,d)^{32}S$ reaction leading to proton-unbound states. If not shown the error is less than the point size. Curves are DWBA predictions for the indicated l values. For the E_x= 9732 keV level, see text (Sec. V B).

mixtures in predominantly $l=1$ and $l=3$ transfers, respectively, for $E_x<9$ MeV (bound states), and with 20% $l=3$ and 10% $l=1$ admixtures for $E_x>9$ MeV (unbound states).

When the J^π value was not previously known the l value or the admixture of l values which fitted best the experimental angular distributions was searched for. In all cases the transitions were considered to proceed by a single l value if the admixture extracted from the analysis was found to be less than the above stated limits.

The angular distributions leading to bound and proton-unbound states are presented in Figs. 3 and 4, respectively, together with the DWBA fits. Some levels for which the extraction of a definite l value from the experimental angular distribution was not possible are presented in Fig. 5. Some deuteron angular distributions which do not have a stripping pattern are presented in Fig. 6. The mechanism leading to the weak population of these states does not seem to be a pure direct one-step process. No attempt was made to analyze these angular distributions. Errors shown in Figs. 2–6 are due to statistics and background substraction only.

V. COMMENTS ON RESULTS

The spectroscopic information obtained in the present work is presented in Tables III–V. In this section we discuss specific points which entered into our conclusions as summarized in the tables.

A. Energy levels

One-hundred and eleven levels were observed in the present work, a number of them for the first time. Their identification with levels of ^{32}S follows from kinematical analysis. The excitation energies are presented in Tables III and IV along

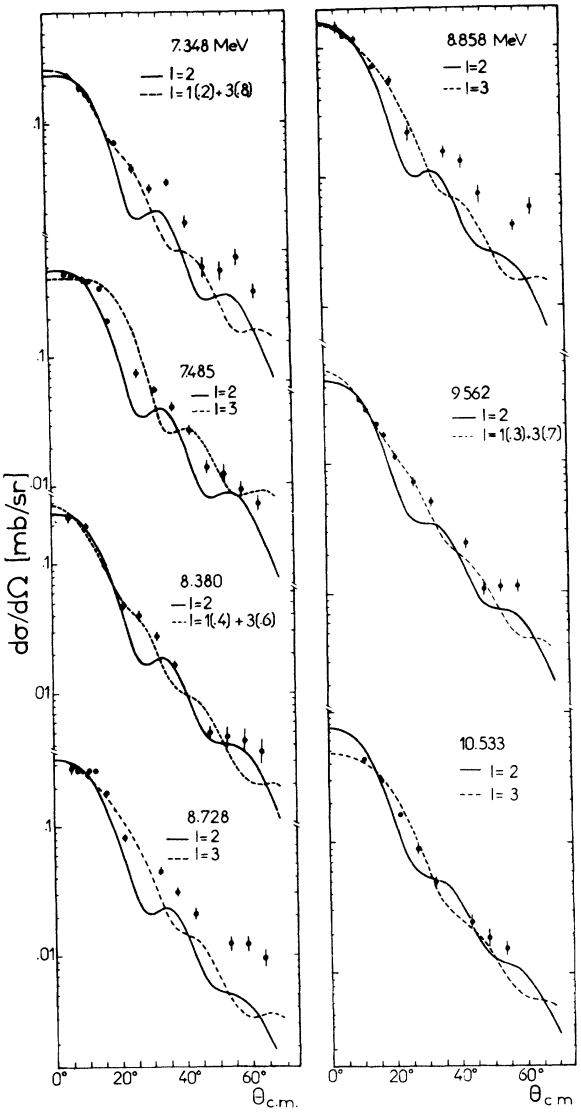

FIG. 5. Angular distributions of the $^{31}P(^{3}He,d)^{32}S$ reaction which do not yield a definite l value.

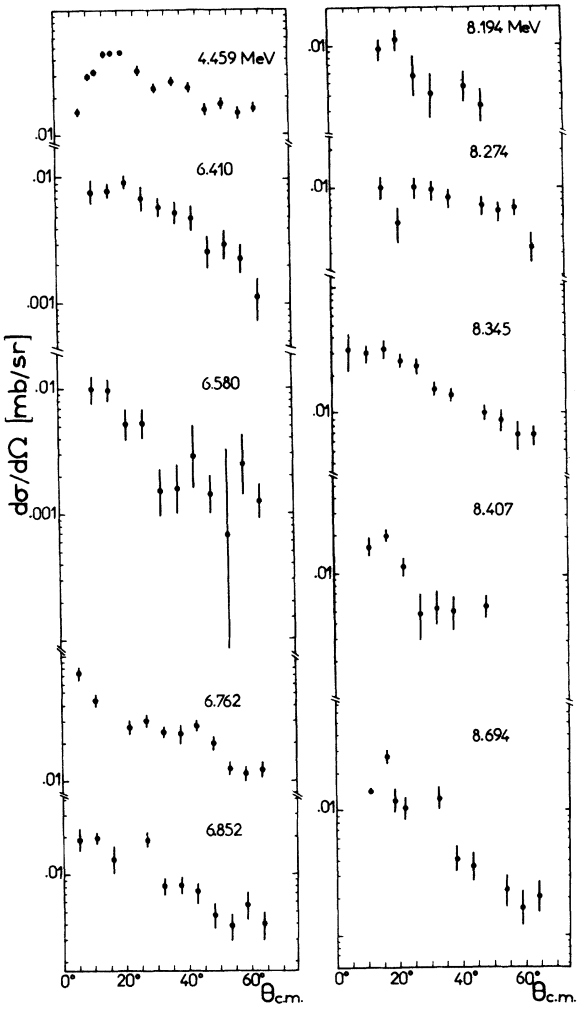

FIG. 6. Angular distributions of the $^{31}P(^{3}He,d)^{32}S$ reaction which do not have a typical stripping pattern.

with values from Ref. 11, from recent high-resolution studies of the $^{33}S(p,d)^{32}S$ (Ref. 6) and $^{34}S(p,t)^{32}S$ (Ref. 7) reactions, and from recent resonance capture studies.[3,20,21]

With the exception of the $E_x = 8790$ keV level, all the proton bound states quoted in Ref. 11 are populated in the stripping reaction (though sometimes weakly). The very weakly populated level $E_x = 6580$ keV is identified with the natural-parity state observed at $E_x = 6581 \pm 3$ keV by Gardner *et al.*[22] in a study at 180° of the $^{32}S(\alpha,\alpha')^{32}S$ reaction. The existence of a doublet of levels around 7.95 MeV, which was suggested by Graue *et al.*,[1] is confirmed. The first component, $E_x = 7950$ keV, is identified with the $J^\pi = 4^-$, $E_x = 7950.0 \pm 0.4$ keV level[20]; the second one, $E_x = 7973$ keV, might be the $E_x = 7.92 \pm 0.07$ MeV level observed in a study of the $^{32}S(p,p')^{32}S$ reaction at 185 MeV, for which the $J^\pi = 3^-$ value was proposed.[23]

The identification of states observed in the present work with resonance levels observed in the $^{31}P(p,\gamma)^{32}S$ and $^{28}Si(\alpha,\gamma)^{32}S$ reactions[3,11,20,21] was also attempted. This identification rests upon two arguments. The first one is the agreement within error limits between the excitation energies obtained from the stripping and the resonance capture reactions. The second argument is the consistency between the J^π or l values obtained from the capture reactions and the orbital momentum transfer values from the stripping reactions.

These identifications are firm up to an excitation energy of about 10.4 MeV but only tentative from there on up to 10.9 MeV. They become quite

TABLE III. Spectroscopic informations and comparison with other data for ^{32}S levels ($E_x < 11$ MeV).

$^{31}P(^3He,d)^{32}S$[a]		G_l ($^3He,d$)		(d,n)	$^{34}S(p,t)^{32}S$[e]		$^{33}S(p,d)^{32}S$[f]		Data from resonance capture reactions				$J^\pi T$ values
E_x (keV)	l_p	25 MeV[b]	12 MeV[c]	7 MeV[d]	E_x (keV)	J^π	E_x (keV)	l_n	E_x (keV)[g]	(α,γ)[h] E_α (keV)	(p,γ)[i] E_p (keV)	J^π[j] T[j]	adopted[k]
0	0	0.65	0.60	0.75	0	0^+	0	2	0			0^+	0^+
2229	2	1.34	1.50	1.51	2230	2^+	2233	0+2	2230.2 ± 0.2			2^+	2^+
3778	0	0.17	0.10	0.15	3778	0^+	3779	2	3778.7 ± 1.0			0^+	0^+
4280	2	0.014			4280	2^+	4284	0+2	4281.6 ± 0.8			2^+	2^+
4463					4459	4^+	4458	2	4458.8 ± 0.6			4^+	4^+
4695	2	0.61	0.37	0.67	4696		4694	0+2	4695.3 ± 0.4			1^+	1^+
5006	3	0.86	0.56	0.92	5007		5004	3	5006.2 ± 0.3			3^-	3^-
5415	2	0.03[l]			5415		5410	2	5412.6 ± 1.0			3^+	3^+
5550	2	0.20	0.16	0.13	5553	2^+	5547	0+2	5548.7 ± 1.1			2^+	2^+
5802	1	0.16	0.14	0.15	5797		5798	1	5797.6 ± 1.0			1^-	1^-
6222	1	0.19	0.15	0.15	6230				6224.3 ± 0.9			2^-	2^-
6413					6417	4^+			6410 ± 2			(1–4)	4^+
6580					6584		(6581)						natural parity[m]
6618	3	0.81	0.65	0.54			6621	3	6621.1 ± 0.3			4^-	4^-
6663	2	0.08		0.10	6662	2^+	6666	0+2	6665.7 ± 0.8			$(1,2)^+$	2^+
6759					6769		6762		6761.7 ± 1.0			$(3^-,4^+,5^-)$	$(3^-,4^+,5^-)$
6851					6851	(4^+)	6852		6852 ± 2			(2–4)	(2–4)
7001	2	0.61	0.45	0.58	7000		7002	0+2	7003.3 ± 1.1			$1^+,1$	$1^+,1$
7116	2	0.99	0.88	0.70	7116	2^+	7116	0+2	7115.8 ± 0.9			$2^+,1$	$2^+,1$
7189	0	0.05	0.08	0.02			7191	0+2	7189.9 ± 1.4			1^+	1^+
7348	1	0.002			7349		7351	2	7348 ± 2				
	+3	+0.007											
	or 2	0.02											$(1-3)^+$ *
7430	1	0.08	0.10	0.09	7415				7434 ± 2			(0–2)$^-$	$1^-,(2^-)$ *
7485	2	0.04					7485	2	7484.8 ± 1.0			(1–3)	$(1-3)^+$ *
	or 3	0.06											
7538	0	0.09	0.08	0.05	7536	0^+	7536	2	7535.5 ± 1.0			$(0,1)^+,1$	$0^+,1$
					7637								
7701	3	0.06			7702				7701.7 ± 1.4			(2–4)$^-$	(2–4)$^-$
7883	1	0.04	0.04	0.04					7877 ± 9			(0–2)$^-$	(0–2)$^-$
					7914								
7950	3	0.10	0.15[n]						7950.0 ± 0.4			4^-[o]	4^-
					7966	4^+	7975						4^+
7973	3	0.09											$(2-4)^-$ *
8123	0	0.18	0.15	0.08	8121				8126.2 ± 1.0			$1^+,1$	$1^+,1$
8194													
8274					8266		8281	2					$\pi = +$
8295	3	0.14	0.15						8294 ± 3			(2)$^-$	$(2-4)^-$ *
8345					8336	2^+	8346	2					$2^+,1$ *
8380	1	0.006					8381						2^-

TABLE III (*continued*)

^{31}P(^{3}He,d)^{32}S[a]		G_l (^{3}He,d)		$\frac{(d,n)}{7\ \text{MeV}}$[d]	^{34}S(p,t)^{32}S[e]		^{33}S(p,d)^{32}S[f]		Data from resonance capture reactions				$J^\pi T$ values
E_x (keV)	l_p	25 MeV[b]	12 MeV[c]		E_x (keV)	J^π	E_x (keV)	l_n	E_x (keV)[g]	(α,γ)[h] E_α (keV)	(p,γ)[i] E_p (keV)	$J^\pi T$[j]	adopted[k]
	+3	+0.009											or
	or 2	0.02											(1–3)$^+$
8407							8408						
							8489						
8499	1	0.15	0.13	0.12					8494 ±2	1767		1$^-$	1$^-$
					8507	0$^+$							0$^+$
8687							8691		8690 ±2	1990		2$^+$	2$^+$
8728	2	0.02[l]			8725		8730		8712 ±15				3$^+$,1 *
	or 3	0.03											
									8790 ±30				
8858	2	0.010			8848		8860		8861 ±2	2187		2$^+$	2$^+$
	or 3	0.014											
9021	3	0.09	0.09		9025				9023 ±2	2371		(1$^-$,2$^+$,3$^-$,4$^+$)	3$^-$ *
9061	1	0.08	0.07	0.10			9061						(0–2)$^-$
									9065 ±2	2419		(2$^+$,3$^-$,4$^+$)	(2$^+$,3$^-$,4$^+$)
							9138						
9169							9170						3$^+$,1 *
					9196	2$^+$							2$^+$
9209	0	0.03							9207 ±1		355	1$^+$,1	1$^+$,1
	+2	+0.08											
9238	1	0.03		0.04					9236 ±2	2614		1$^-$	1$^-$
9255	2	0.07			9252								2$^+$,1 *
9292	0	0.03							9290 ±1		439	1	1$^+$ *
	+2	+0.02											
9395	1	0.31	0.36	0.23					9389 ±1		541	2$^-$	2$^-$
9469					9468				9464 ±1	2878	619	2$^+$	2$^+$
9493	1	0.05		0.06					9486 ±1	2901	642	1$^-$	1$^-$
9562	1	0.001											2$^-$
	+3	+0.002											or
	or 2	0.003											(1–3)$^+$
9652	2	0.06			9650	2$^+$	9655		9650 ±1		811	2$^+$	2$^+$,1 *
									9660 ±1		821	1	1
									9711 ±1	3159	874	2$^+$	2$^+$
9732[p]	3	0.17							9723 ±1		888	(3$^-$)	(3)$^-$ *
	1	0.11		0.08					9730 ±1		895	(1$^-$,2$^+$)	1$^-$ *
							9785						
9823	3	0.20			9820				9817 ±1		984	(2$^+$,3$^-$)	3$^-$ *
9853	1	0.04		0.02									(0–2)$^-$ *
9893	2	0.05					9886		9887 ±1		1057	(1,2)	(1,2)$^+$ *
					9920	2$^+$			9919 ±1		1090		2$^+$

TABLE III (*continued*)

$^{31}P(^3He,d)^{32}S$[a]		G_l			$^{34}S(p,t)^{32}S$[e]		$^{33}S(p,d)^{32}S$[f]		Data from resonance capture reactions					
		$(^3He,d)$		(d,n)						(α,γ)[h]	(p,γ)[i]			$J^\pi T$ values
E_x (keV)	l_p	25 MeV[b]	12 MeV[c]	7 MeV[d]	E_x (keV)	J^π	E_x (keV)	l_n	E_x (keV)[g]	E_α (keV)	E_p (keV)	$J^\pi{}_i T_i$	adopted[k]	
9955	1	0.03					9947		9949			1121	1	1^- *
9985	3	0.24					9976		9978	±1		1151	3^-	3^-
									9983	±1		1155	2^+	2^+
10021	3	0.02												$(2-4)^-$*
10072	1	0.44		0.31					10072	±2		1247	$2^-,0+1$[q]	$2^-,0+1$
10098									10102	±2		1279	(2–4)	(2–4)
									10219	±2		1399	3^+	3^+
10223	3	0.70							10222	±2	3739	1402	$3^-,0+1$	$3^-,0+1$
									10225	±2		1405	$(0-2)^-$	$(0-2)^-$
									10230	±2		1411	1^+	1^+
10257	3	1.30							10256	±2		1437	$4^-,0+1$	$4^-,0+1$
					10276	4^+								4^+
10287	3	0.26							10287	±2	3814	1469	$3^-,0+1$	$3^-,0+1$
									10289	±2		1472	$2^-,0+1$	$2^-,0+1$
									10291	±2	3827	1474	2^+	2^+
10330	1	0.17		0.08					10331	±2	3877	1515	1^-	1^-
10368	2	0.06			10370	2^+			10369	±2		1555	$2^+,1$	$2^+,1$
10395	3	0.36							10395	±2		1581	$4^-,0+1$	$4^-,0+1$
				0.07[r]					10399	±2		1585	0^-	0^-
10428														
									10509	±1		1699	(1–3)	(1–3)
					10530				10531	±8	4096		2^+	2^+
10533	2	0.04												$(1-3)^+$
	or 3	0.05												or (2–4)-
									10556	±1		1747		
									10573	±1		1764		
									10603	±1		1796		
10624	3	0.08							10634	±8	4210		$(1^-,3^-)$	3^- *
									10696	±1		1892	2^+	2^+
10698	1	0.48							10700	±1	4299	1896	1^-	1^-
									10756	±1		1954	$2^+3,4^+$	$2^+.3,4^+$
10777	1	0.26							10779	±1		1966	$1^-,2^+$	1^-*
					10780	2^+								2^+
									10785	±1		1984	$1^-,2^+$	$1^-,2^+$
									10792	±1		1991	$1^-,2^+$	$1^-,2^+$
					10823	2^+								2^+
10826	1	0.22							10827	±1		2027	$1^-,2^+$	$1^-,0+1$*
10977	(1)[s]	0.12												1^-[s], 0+1*

TABLE III (*continued*)

[a] Present work. The accuracy is ±5 keV for $E_x \leq 9$ MeV, and ±10 keV for higher excited states.
[b] Present work.
[c] Reference 1.
[d] Reference 5.
[e] Reference 7. The accuracy is ±5 keV for $E_x \leq 8$ MeV and ±8 keV for higher excited states.
[f] Reference 6.
[g] The excitation energies reported in this column are from resonance capture studies (Refs. 3, 11, 20, and 21) except for the levels $E_x = 8712 \pm 15$ and 8790 ± 30 keV the information about which being from Refs. 1 and 11, respectively.
[h] For $E_\alpha \leq 3814$ keV the resonance energies are from Ref. 21; the higher resonance energies are from Ref. 11.
[i] The proton resonance energies are from Ref. 11 except for the $1247 \leq E_p$ (keV) ≤ 1585 range in which they are from Ref. 3.
[j] These values are taken from Refs. 3, 11, 20, and 21.
[k] New conclusions from the present work are indicated by an asterisk.
[l] A $1d_{5/2}$ transfer was used to get the spectroscopic strength.
[m] Reference 22.
[n] This strength is for the two members of the 7950–7973 keV doublet which were not resolved in Ref. 1.
[o] Reference 3.
[p] This apparently unique peak consists in fact of two levels (see text, Sec. V B).
[q] The 10072–10289 , 10222–10287, 10256–10395, and 10826–10977 keV pairs of levels are suggested as members of isospin mixed doublets (see Ref. 3 and text, Sec. V D).
[r] See text, Sec. V B.
[s] See text, Sec. V B and V D.

tenuous for higher excitation energies due to the incomplete deuteron angular distributions (see Sec. III) and to the scarce spectroscopic information about the resonance levels in this energy range. The energy values from the present work (Tables III and IV, column 1) will be used throughout the following discussion in this paper.

B. l values and spectroscopic strengths

For the many transitions measured here to states of previously known J^π values, the l values extracted from our analysis are consistent with the prior assignments. The quality of the agreement between the DWBA curves and the data can be judged from Figs. 3 and 4.

For the levels of previously unknown spin and parity at $E_x = 7348$, 7485, 8380, 8728, 8858, 9562, and 10533 keV the shapes of an $l = 2$ transfer and those of an $l = 3$ transfer pure or mixed with $l = 1$ yield similar fits to the angular distributions (Fig. 5). However, the ambiguity can be removed for four of these levels by the use of information from other reactions: The $l = 2$ assignment was adopted for the $E_x = 7348$ and 7485 keV levels from a comparison with the ^{33}S(p, d)^{32}S data,[6] for the $E_x = 8728$ keV level from the identification with a $J^\pi = 3^+$, $T = 1$ state of ^{32}S (see Sec. V D) and for the $E_x = 8858$ keV level from the identification with the $E_\alpha = 2187$ keV resonance of the ^{28}Si(α, γ)^{32}S reaction.[21] These l values are underlined in Table III.

As mentioned, only unnatural-parity states in ^{32}S can be populated by mixed transfer of two different l values. Only two 1^+ states, $E_x = 9209$ and 9292 keV, are observed to be populated by significantly mixed $l = 0 + 2$ transitions. The lower lying 1^+ states are populated by essentially pure $l = 2$ transitions. This is in contrast to the situation observed in the ^{29}Si(^{3}He, d)^{30}P reaction[15] in which most 1^+, $T = 0$ states were observed to be populated by mixed $l = 0 + 2$ transitions. This difference can be due to the fact that the filling of the $2s_{1/2}$ subshell is more complete in the ^{31}P nucleus than in the ^{29}Si nucleus.

In the present work more $l = 3$ transitions are observed than is the case in the (d, n) reaction.[5] This can be explained because the matching of angular momentum in the (d, n) reaction at 7 MeV enhances $l = 1$ and hinders $l = 3$ transfers around $E_x = 10$ MeV, whereas for the (^{3}He, d) reaction at 25 MeV, the $l = 1$ and 3 transfers have rather similar maximum cross sections. A peak which is observed around 9730 keV in the (d, n) as well as in the (^{3}He, d) reactions yields an example of such a different population through the two stripping reactions. A first analysis of the (^{3}He, d) angular distribution led to a $l = 2$ assignment which conflicts with the $l = 1$ result from the (d, n) experi-

TABLE IV. Spectroscopic information from the $^{31}P(^3He, d)^{32}S$ reaction for ^{32}S levels with $E_x > 11$ MeV.

E_x (keV) [a]	l_p	G_j	J^π, T	E_x (keV) [a]	l_p	G_j	J^π, T
11 008				11 823			
11 091	3	0.06	$(2-4)^-$	11 861			
11 198	3	0.10	$(2-4)^-$	11 876			
11 233				11 900			
11 256				11 936	3	0.06	$(2-4)^-$
11 366				11 955			
11 438				12 002			
11 475				12 044 [b]	3	0.14	$4^-, 1$
11 504				12 160	(2)	(0.18)	$((1-3)^+)$
11 551				12 196			
11 583				12 235	(2)	(0.06)	$((1-3)^+)$
11 603				12 308			
11 623				12 340			
11 660				12 362			
11 690				12 393			
11 720				12 426			
11 750				12 465			
11 783				12 491			
11 806							

[a] ±10 keV.

[b] This level is identified with the resonance level 12 044 ± 4 keV, $J^\pi = 4^-$, $T = 1$, observed at $E_p = 3283$ keV in the $^{31}P(p, \gamma)^{32}S$ reaction (Ref. 9).

ment. However, this discrepancy can be removed by assuming that the two $E_x = 9723$ and 9730 keV levels, $J^\pi = (3^-)$ and $(1^-, 2^+)$, respectively, which are known from previous proton capture work[11] are populated but not resolved in the present work, whereas only the $E_x = 9730$ keV level is significantly populated in the (d, n) reaction. An adjusted superposition of $l = 1$ and 3 contributions (simulating a $l = 2$ transfer shape) was found to reproduce the $(^3He, d)$ angular distribution of the two unresolved levels (Fig. 4): This permits the reconciliation of the results of the two stripping reactions.

Another example of different population is found with the close doublet of levels ($E_x = 10395$ keV, $l = 3$, $J^\pi = 4^-$ and $E_x = 10399$ keV, $l = 1$, $J^\pi = 0^-$) which were observed in the $^{31}P(p, p)^{31}P$ reaction.[3] Due to the hindrance of $l = 3$ transfers quoted above, only the $E_x = 10399$ keV level is observed in the (d, n) reaction.[5] By contrast, only the $l = 3$ transfer is observed in the $(^3He, d)$ reaction, indicating a spectroscopic strength more important for the first component of the doublet than for the second one.

Deuterons leading to ^{32}S levels at 10777, 10826, and 10977 keV are mixed at forward angles with deuterons leading to ^{13}N levels at 3509 and 3547 keV (see Sec. III), so that angular distributions could be obtained only from $\theta_{lab} = 15°$ for the 10777 and 10826 keV levels, and from $\theta_{lab} = 25°$ for the 10977 keV one. Despite the missing angles at 5° and 10°, the shape of an $l = 1$ transfer yields a much better fit to the angular distributions of the 10777 and 10826 keV levels than the shapes of $l = 2$ or $l = 3$ transfers. For the 10977 keV level, while $l = 2$ or $l = 3$ transfers cannot be definitely excluded, the $l = 1$ shape best fits the available experimental points. Also the experimental points of the angular distributions of the 10977 keV level can be superimposed almost exactly with those of the more complete angular distribution of the 10698 keV level, for which an $l = 1$ transfer has been unambiguously established. Thus an $l = 1$ transfer is probable for the 10977 keV level, but due to the lack of data at more forward angles than $\theta_{lab} = 25°$ this assignment is given in parentheses in Table III and Fig. 4(b).

The spectroscopic strengths G_{l_j} which are presented in Table III were extracted with DWBA calculations based on the parameters of Table I under the assumption of a $1d_{3/2}$, $2p_{3/2}$, or $1f_{7/2}$ transfer (with some exceptions quoted in Tables III and IV). They are compared in these tables with the most extensive of the other available data. For the $T = 1$ states, the G_{l_j} values from (d, n) are smaller than the values from $(^3He, d)$. This point was already discussed in Ref. 24.

C. Spin and parity assignments

Most of the J^π values presented in the last column of Table III are from Ref. 11 and from the

recent pickup reactions.[6,7] New information from the present work is indicated by an asterisk in Table III. Part of this new information follows from the identification between resonance and stripping levels: In particular, natural parity comes from the identification with a resonance level of the ^{28}Si(α, γ)^{32}S reaction. Some information was gathered also through isospin assignments as discussed in Sec. V D. For two levels the limitations of the J^{π} values are obtained from other sources, as it is discussed in the following:

E_x = 7430 keV level: The J^{π} value of this l = 1 state is restricted to $(0-2)^-$. A ground-state γ-ray transition was observed in a recent study[25] of the ^{31}P(^{3}He, $d\gamma$)^{32}S reaction. Therefore the $J^{\pi} = 0^-$ value must be rejected. The $J^{\pi} = 1^-$ value seems more likely since the level is strongly populated in the ^{28}Si(^{6}Li, d)^{32}S reaction.[26] However, the $J^{\pi} = 2^-$ value cannot be definitely rejected because unnatural-parity states are also populated, even though much more weakly, in the (^{6}Li, d) reaction, therefore $J^{\pi} = 1^-(2^-)$.

E_x = 8295 keV level: The l = 3 proton transfer leads to $J^{\pi} = (2-4)^-$. A tentative $J^{\pi} = 2^-$ assignment was made in Ref. 11 on the basis of the report[27] of a 60% ground-state transition.[27] However this ground-state transition was not observed in the (^{3}He, $d\gamma$) reaction.[25] Therefore $J^{\pi} = (2-4)^-$.

D. Isospin assignments

Isospin values of T = 1 were already assigned to the E_x = 7001, 7116, 7538, 8123, 9209 keV (Ref. 11), 10368 keV (Ref. 3), and 10244 keV levels (Ref. 10); evidence of T mixing in the E_x = 10072,

TABLE V. A comparison of spectroscopic information in ^{32}P and ^{32}S leading to T = 1 assignment to some ^{32}S levels. The information is from Refs. 4, 29, and 30 for ^{32}P and from the present work and Ref. 10 for ^{32}S.

^{32}P		^{32}S		$(2J_f+1)S_n$ l_n				$(2J_f+1)S_p$ l_p				$E_x(^{32}S) - E_x(^{32}P)$ (keV)
E_x (keV)	J^{π}	E_x (keV)	J^{π}	0	1	2	3	0	1	2	3	
0	1^+	7003.3	1^+	<0.07		3				2.6		7003
78.1	2^+	7115.8	2^+			4.7				4.0		7038
512.9	0^+	7535.5	0^+	0.32				0.36				7023
1149.8	1^+	8126.2	1^+	0.53				0.72				6976
1323.2	2^+	8345		no stripping pattern				no stripping pattern				7022
1754.4	3^+	8728				(0.07)				0.08		6974
2177.6	3^+	9169		weakly excited				weakly excited				6991
2218.9	2^+	9255				0.33				0.28		7036
2229.8	1^+	9209	1^+	0.13		0.40		0.12		0.32		6979
2657.7	2^+	9650	2^+			0.20				0.24		6992
2741.4	1^+			0.003		0.04						
3004.4	3^+					0.22						
3149.3	4^+											
3264.0	2^-	10072 [a]	2^-		1.1				1.76			6840 [b]
		10289	2^-									
3321.5	3^-	10223 [a]	3^-				3.1				2.8	6920 [b]
		10287	3^-								1.0	
3443.0	4^-	10256 [a]	4^-				7.0				5.2	6883 [b]
		10395	4^-								1.5	
3444.0	$(0-2)$	10368	2^+			c				0.24		6924
3797.3	3^-						0.13					
3875	$(1-3)^+$					0.28						
3988.7	$1^+, 2^+, 3$											
4007.1	2^-				0.33		0.62					
4036.2	1^-	10826	1^-		1.30				0.88			6843
		10977	(1^-)						(0.48)			
4158	$(2-4)^-$		4^-				0.18					
5081.5	$2^-, 4^-$	12044									0.14	6962

[a] T-mixed doublet of levels (Ref. 3).
[b] Estimated value from the calculation of the unperturbed T = 1 level energy (Ref. 3).
[c] Masked by the strongly populated E_x = 3443 keV level.

10223, 10257, 10287, 10289, and 10395 keV levels comes from their electromagnetic properties.[3]

In the present work $T=1$ assignments were made to the $E_x=8345$, 8728, 9169, 9255, and 9652 keV levels (Table V) on the basis of the fulfillment of at least one of the two following criteria:

(a) The energy difference between the ^{32}S level and its ^{32}P parent must remain nearly constant, keeping in mind that the mean energy difference is not the same for even- and odd-parity states, as previously noted for $A=32$ (Ref. 3) and $A=36$ (Ref. 28) nuclei.

(b) Insofar as they can be extracted properly from the one-proton and one-neutron stripping reaction data on ^{31}P, spectroscopic factors of corresponding states in ^{32}S and ^{32}P should be the same. As can be seen in Table V they are in mutual agreement within 20% except for the $J^\pi=2^-$ levels for which the deviation reaches 40%.

No unique level could be identified as the analog of the strongly excited ^{32}P state at $E_x=4036$ keV. However, assuming that the analog state is split into two T-mixed components as it is in the case for the known analogs of other odd-parity ^{32}P states,[3] the two ^{32}S levels $E_x=10826$ keV, $l=1$ and 10977 keV, $(l=1)$ should constitute the members of such a doublet. Their spectroscopic factors add to 1.36, which compares well with the value of 1.30 obtained for the ^{32}P state. Assuming also that the "true" position of the analog state is the centroid of the energies of the two components weighted by their spectroscopic factors, the value $E_x=10879$ keV is obtained: The energy difference between the analog and the parent levels compares very well with the energy difference between the members of the other $l=1$ pair. Then the 10977 keV could be definitely assigned $l=1$. On these grounds the two $E_x=10826$ and 10977 keV levels were assigned $T=0+1$.

The analogs of the $E_x=2741$ and 3797 keV states of ^{32}P are expected around 9740 and 10700 keV, respectively, using the mean energy difference for even- and odd-parity states. They should be masked by the more strongly populated levels at $E_x=9732$ and 10698 keV.

Using the criteria defined above it was not possible to identify in ^{32}S the analogs of the other ^{32}P states presented in Table V.

VI. COMPARISON WITH SHELL-MODEL CALCULATIONS

In this section the excitation energies and spectroscopic factors measured for positive-parity states in ^{32}S are discussed in the light of results of a recent shell-model calculation for $A=28$–38 nuclei.[31] The theoretical predictions were obtained by diagonalizing in the complete $d_{5/2}$-$s_{1/2}$-$d_{3/2}$ basis space a Hamiltonian which reproduces the single-hole spectrum of $A=39$ and simultaneously yields a root mean square (rms) best fit to a selected set of known level energies in the $A=32$–38 region. The spectroscopic factors $S(j)$, $^{31}\mathrm{P}\rightarrow{}^{32}\mathrm{S}$, for the lowest six eigenstates of each J, T combination in $A=32$ are available from these calculations and are compared to the present data in Table VI, simultaneously with a comparison of calculated and observed excitation energies.

There is a natural division, in both the theoretical and experimental results, between the total spectroscopic strength for single-nucleon transfer within a given major shell and the distribution of that strength over the individual single-particle orbits and specific final states of the residual system. To facilitate comparisons between individual states in the model and observed spectra in Table VI, the experimentally determined spectroscopic factors of Table III were multiplied by a factor of 0.75. As will be discussed further in Sec. VII, this serves to produce an equality between the observed total spectroscopic strength for the *sd* shell and the total strength predicted for the observed states.

In arriving at a judgement of whether a significant discrepancy exists between the calculated and measured spectroscopic factor for a given level, consideration must be given both to the internal uncertainties of the standard DWBA analysis (for instance, how well are the dependences of the cross sections upon l_j, Q value, etc..., described) and to the possibility that various reaction mechanisms other than the simple one-step direct process may contribute to the observed cross sections, thus rendering the usual DWBA analysis partially invalid. These sorts of problems in the determination of experimental spectroscopic factors contribute uncertainties which are both multiplicative and additive; it is our estimate that the minimum uncertainty in an individual spectroscopic factor is in the present case at least 0.05 single-particle unit. If the results of Table VI are inspected in the context of this criterion it can be seen that the spectroscopic factors predicted for states below 7 MeV are each in agreement with the present experimental values. It follows that, relative to the ground state of ^{31}P, the single-particle aspects of the lowest eight states of ^{32}S which are embodied in the model wave functions are consistent with experiment to the currently achievable level of discrimination.

Underlying the comparison of individual spectroscopic factors is the question of whether the

TABLE VI. Comparison of experimental and calculated excitation energies and spectroscopic strengths.

Shell-model calculations $G_{lj}\times100$						Present work $G_l\times75$ [a]					$E_{x_{exp}}-E_{x_{calc}}$ (keV)
E_x (keV)	J^π_ν	T	$2s_{1/2}$	$1d_{3/2}$	$1d_{5/2}$	E_x (keV)	J^π	T	$l=0$	$l=2$	
0	0^+_1	0	46			0	0^+	0	48		0
2 398	2^+_1	0		105.3	7.75	2 229	2^+	0		99	−169
3 839	0^+_2	0	8.88			3 778	0^+	0	12		−61
4 169	2^+_2	0		2.0	0.45	4 280	2^+	0		1.0	111
4 919	1^+_1	0	0.00	46.1		4 695	1^+	0		45	−224
5 369	3^+_1	0			4.03	5 415	3^+	0		2.2	46
5 459	2^+_3	0		9.25	0.23	5 550	2^+	0		15	91
6 949	2^+_4	0		0.09	11.1	6 663	2^+	0		6	−286
7 109	0^+_3	0	0.08								
7 109	3^+_2	0			0.68						
7 119	1^+_1	1	0.88	37.40		7 001	1^+	1		45	−118
7 139	1^+_2	0	6.51	0.90		7 189	1^+	0	3.7		50
7 189	0^+_4	0	0.02								
7 239	0^+_1	1	4.88			7 538	0^+	1	6.7		299
7 279	2^+_1	1		65.9		7 116	2^+	1		73	−163
7 509	2^+_5	0		0.01	0.05						
8 079	2^+_2	1		1.10		8 345	2^+	1			266
8 109	2^+_6	0		0.14	1.33						
8 239	1^+_2	1	11.50	1.88		8 123	1^+	1	13		−116
8 249	0^+_5	0	0.03			8 507 [b]	0^+ [b]	0			258
8 319	3^+_3	0			0.46						
8 499	1^+_3	0	0.20	0.05							
8 729	3^+_1	1			8.54	8 728	3^+	1		1.5	−1
8 759	1^+_4	0	0.02	3.23							
8 959	3^+_4	0			2.21						
9 069	2^+_3	1		1.14	9.74	9 255	2^+	1		5.2	186
9 179	1^+_3	1	0.10	1.38		9 209	1^+	1	2.2	5.9	30
9 239	3^+_2	1			4.29	9 169	3^+	1			−70
9 579	0^+_6	0	0.29								
9 769	2^+_4	1		0.66	6.16	9 650	2^+	1		4.4	−119
9 779	1^+_5	0	0.17	0.40		9 292	1^+	0	2.2	1.5	−487
9 879	3^+_5	0			0.89						
9 949	3^+_3	1			2.61						
10 019	1^+_4	1	0.85	3.34							
10 069	3^+_6	0			2.36						
10 319	1^+_6	0	0.25	0.08							
10 379	2^+_5	1		3.00	1.00	10 368	2^+	1		4.4	−11
10 609	1^+_5	1	0.04	1.65							

TABLE VI. *(continued)*.

Shell-model calculations $G_{lj}\times100$						Present work $G_l\times75$ [a]					$E_{x_{exp}}-E_{x_{calc}}$ (keV)
E_x (keV)	J^π_ν	T	$2s_{1/2}$	$1d_{3/2}$	$1d_{5/2}$	E_x (keV)	J^π	T	$l=0$	$l=2$	
10 609	3^+_4	1			2.00						
10 669	0^+_2	1	1.98								
10 749	2^+_6	1			2.00						
10 959	1^+_6	1	1.58	0.40							
11 179	3^+_5	1			2.03						
11 519	3^+_6	1			0.37						
11 799	0^+_3	1	0.51								
13 699	0^+_4	1	0.01								
14 349	0^+_5	1	0.08								
14 599	0^+_6	1	0.03								

[a] The 75 (instead of 100) coefficient is due to a renormalization factor which serves to produce an equality between the total spectroscopic strength of the experimental levels which can be reasonably identified with calculated levels and the total spectroscopic strength predicted for these levels (see text, Secs. VI and VII).

[b] Reference 7.

theoretical results correctly account for the distribution of the spectroscopic strength among the active shell-model orbits. In the present data the relative $l=0$ to $l=2$ strength can be reliably extracted because the $J^\pi=\frac{1}{2}^+$ ground state of ^{31}P eliminates mixing of l values for all but the $J^\pi=1^+$ states. In addition, the characteristics of the reaction process are such that the presence of a $l=0$ contribution less than 10% in a predominantly $l=2$ distribution can be detected and extracted (see Sec. IV). This latter feature allows, for example, the predicted vanishing of the $l=0$ strength of the lowest $J^\pi=1^+$, $T=0$ level to be experimentally verified to high accuracy. The good agreement between calculated and observed (as multiplied by 0.75) spectroscopic factors for the individual low-lying states implicitly confirms that the predicted overall $s_{1/2}$ to $d_{3/2}$ strength is correct, since these transfers dominate the transfer process in this region.

The other relevant aspect of general configuration mixing of this region of the nuclear table involves relative $d_{3/2}$ to $d_{5/2}$ spectroscopic strength and, hence, the degree of excitation of the $d_{5/2}$ subshell. Since most of the $l=2$ strength in the present reaction is manifested in the $J^\pi=2^+$ states and it is not possible to distinguish from the present data the contributions of the simultaneously allowed $d_{3/2}$ and $d_{5/2}$ transfers, it is not easy to test the predicted values of $d_{5/2}$ strength. The essential "hole" nature of the $d_{5/2}$ orbit in this region creates a further problem with the DWBA analysis itself. Small but appreciable amounts of $d_{5/2}$ strength are predicted for two of the first four 2^+ states and for the lowest 3^+ state. All that can be inferred from the experimental results is that these predictions are not strongly at variance with the data.

In the region of excitation energy above 7 MeV several states are predicted to have spectroscopic factors large enough to make possible clear tests with the experimental results. The lowest observed $T=1$ states, the 1^+-2^+ analogs of the ^{32}P ground-state doublet, have extracted strengths about 10% larger than the predicted $d_{3/2}$ values. The predicted $l=0$ strengths of the second 1^+, $T=0$, first 0^+, $T=1$, and second 1^+, $T=1$ states are confirmed by the experimental results for the levels observed at $E_x=7189$, 7538, and 8123 keV, respectively.

Beyond these levels, appreciable $l=2$ strength (mostly $d_{5/2}$) is predicted for the ($T=1$) first and second 3^+, third, fourth, and fifth 2^+ states. While there are several plausible correspondences between these model levels and observed levels, as delineated in Table VI, the agreement is not so clear as for the more strongly excited, lower-lying levels. The observed strengths for these higher excitation states are generally smaller than the calculated values, which suggests that the model predictions for $d_{5/2}$ strength, and hence for the degree of $d_{5/2}$ core excitation are too

large.

Implicit in this discussion of the detailed comparison of calculated and observed spectroscopic factors is the agreement between calculated and observed excitation energies. As can be noted in Table VI, the typical deviation of the calculated energies from the experimental energies is about 200 keV. Thus not only do the shell-model wave functions in general give a correct account of the sequence and magnitudes of the individual spectroscopic factors, but the Hamiltonian which yielded these wave functions also correctly yields the energies of the individual states. At higher excitation energies the deviations between calculated and observed energies increase, in parallel to the situation with spectroscopic factors just noted. There is an inherent problem in carrying model-experimental comparisons to the higher states of a given J, T value. The level spacing between the model states decreases and the mixing of different characteristics of these states becomes very sensitive to the otherwise unimportant details of the Hamiltonian. In addition, the observed spectrum is complicated still further by the emergence of additional levels of the same J^{π}, T value which originate from configurations lying outside the model space. In combination, these difficulties make the decrease in quantitative agreement between theory and experiment in the 8–10 MeV region of excitation unsurprising.

VII. COMPARISON WITH THE SUM-RULE LIMITS

The distribution of the spectroscopic strength among the various levels is displayed on Fig. 7. Except for the $l=1$, $T=0$ case, most of the observed strength is concentrated into a few levels: thus 100%, 85%, 85%, 50%, and 95% of the ($l=1$, $T=1$), ($l=2, T=0$), ($l=2, T=1$), ($l=3, T=0$), and ($l=3, T=1$) observed strengths are carried by two levels or doublets of T-mixed levels.

Various partial summations of the spectroscopic strengths observed and calculated for stripping to the levels of ^{32}S are presented in Table VII. Columns 4 to 8 of this table indicate, respectively: (4) The subtotals of spectroscopic strengths as extracted from the experimental cross sections with the DWBA calculations based on the optical model and bound-state parameters presented in Table I; (5) the same experimental numbers multiplied by 0.75; (6) the subtotals from all of the calculated model states (6 of each J, T); (7) partial sums when the model totals are restricted to those levels whose experimental counterparts are reasonably known; (8) the sum-rule limits from the simple single-particle model. The following sum-

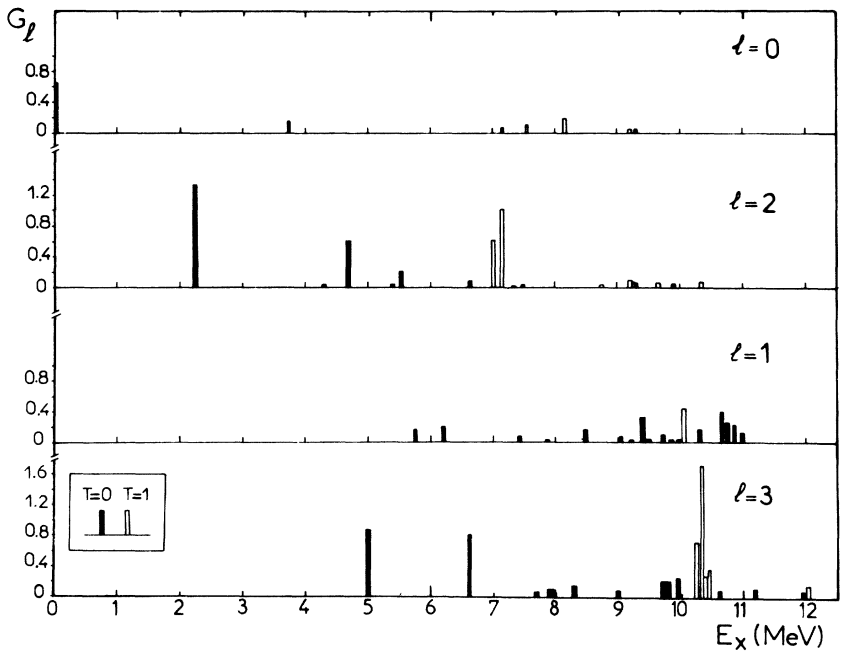

FIG. 7. Distribution of the spectroscopic strengths from the ^{31}P(^{3}He,d)^{32}S reaction. Solid bars indicate $T=0$ transitions, and open bars $T=1$ transitions.

TABLE VII. Summed spectroscopic strengths from the $^{31}P(^{3}He,d)^{32}S$ reaction, and comparison with sum-rule predictions.

		Present work					
		Number			Shell model		Sum-rule
nlj	T	of levels	ΣG_l	$(\Sigma G_l)\times 0.75$ [a]	ΣG_{l_j} [b]	ΣG_{l_j} [c]	limit
$1d_{5/2}$	0	1	0.03	0.02	0.32	0.24	0
$1d_{5/2}$	1	1	0.02	0.02	0.37	0.25	0
$2s_{1/2}$	0	4	0.90	0.67	0.62	0.62	1
$2s_{1/2}$	1	3	0.30	0.22	0.23	0.17	0
$1d_{3/2}$	0	9	2.33	1.73	1.68	1.64	2
$1d_{3/2}$	1	6	1.83	1.36	1.20	1.10	2
all $s+d$	0	14	3.26	2.42	2.62	2.50	3
all $s+d$	1	10	2.15	1.60	1.80	1.52	2
$1f_{7/2}$	0	14	3.16	2.35			4
$1f_{7/2}$	1	5	2.76	2.05			4
$2p_{3/2}$	0	15	2.08	1.55			2
$2p_{3/2}$	1	3	0.78	0.58			2

[a] As to the 0.75 coefficient, see text (Secs. VI and VII).
[b] The sum includes the 48 states of each JT (Table VI).
[c] The sum includes only the states of Table VI corresponding to an experimental level.

rule relations between the spectroscopic strengths from proton stripping on a target with N neutrons and Z protons and the numbers of neutron and proton holes for a particular orbit l_j in the target have been established[2]:

$$\sum G_{l_j}(T=1) = \frac{1}{(N-Z+1)} \langle \text{neutron holes} \rangle_{l_j},$$

$$\sum G_{l_j}(T=0) = \langle \text{proton holes} \rangle_{l_j} - \frac{1}{(N-Z+1)} \langle \text{neutron holes} \rangle_{l_j}.$$

A. Even-parity states

The measured results for the even-parity levels can be discussed both in the context of the limits of the simple individual particle model and in the context of the present mixed configuration shell model (MCSM). The MCSM results are related to the sum-rule limits by the constraint that the number of total sd-shell holes is nine (four for neutrons and five for protons). The differences between the MCSM predictions and the sum-rule limits from the single-particle model are evidenced in Tables VII (for proton transfer only) and VIII (for proton and neutron transfers). They are due to several reasons. First, the calculations predict that there exists considerable vacancy in the $d_{5/2}$ and $s_{1/2}$ orbits compared to the zero-order estimate (Table VIII). The conservation of particles within the model space then requires a corresponding decrease in vacancy in the $d_{3/2}$ orbit. Secondly the calculations predict that 10 to 15% of the proton spectroscopic strength is distributed over the many hundred levels higher in energy than the first six levels of each J, T which have been explicitly calculated. In addition, if the calculated summed strength is restricted to the only levels which can be clearly identified with observed levels, thus the predicted summed strength is reduced by still another 10%.

The $l=0$ and $l=2$ experimental spectroscopic strengths sums taken from the results presented in Table III exceed the sd-shell limit of five by almost 10%, and the predicted sums from the MCSM calculations by considerably more. The sum-rule limits for the sd shell can be superseded if there exists excitation of sd-shell nucleons in the ground state of ^{31}P into the fp shell, for example. While there indeed may exist such $sd \rightarrow fp$ excitations in ^{31}P, the reliability of the absolute normalization of the spectroscopic factors does not seem great enough to make the 10% discrepancy between the simple limits and the experimental value a meaningful foundation for such a conclusion. In fact the agreement between the experimental sum and the simple limit is close to "good" within the criteria adopted in Sec. VI to evaluate agreement in spectroscopic strengths.

The quite different view which results from comparison of the data to the MCSM predictions emerges as follows: Consideration is restricted to the 19 observed levels which were associated with specific model levels in Table VI. This restriction only reduces the total observed strength from 5.41 to 5.38. This value, in turn, exceeds

TABLE VIII. Number of *sd*-shell particles and holes in the ground state of ^{31}P predicted by the mixed configuration shell-model calculations.

	Number of particles		Number of holes		
nlj	mixed configuration shell model	single-particle model	mixed configuration a	shell model b	single particle model
$1d_{5/2}$	10.24	12	1.76	1.41	0
$1d_{3/2}$	2.23	0	5.77	5.51	8
$2s_{1/2}$	2.53	3	1.47	1.30	1
Σ	15	15	9	8.22	9

[a] From occupation numbers.
[b] From the spectroscopic strengths restricted to six states of each *JT*.

the predicted total for these same 19 levels by 35%. If this 35% discrepancy is considered to be significantly outside the limits of the uncertainties inherent in the DWBA, it would indicate that the combined predicted effects of configuration mixing and fragmentation to higher excitation energies are too large. However, while each individual component in the DWBA which underlies the absolute normalization of the spectroscopic strength seems better determined than 30%, it is still conceivable that the combined uncertainties could still account for a net deviation of such a magnitude. Hence we are reluctant even here to draw firm conclusions about the correctness of the shell-model calculations on the basis of the absolute normalization of experimental spectroscopic strengths. Accordingly, the summed values of the experimental spectroscopic strengths are renormalized so that the sum of observed *sd*-shell strength for the 19 levels mentioned equals the sum of strength predicted for the same "observed" levels, as listed in Table VII. This reduction factor, 0.75, leads to the values quoted in Table VI.

The comparison of the renormalized sums to the MCSM predictions shows good agreement between experiment and theory for the relative $l=0$ to $l=2$ strength. Thus the predicted degree of excitation of the $s_{1/2}$ orbit seems well verified. The relative $d_{5/2}$ to $d_{3/2}$ sums are in discrepancy, however. A significant portion of this discrepancy is due to the fact that the experimental values assume $d_{3/2}$ transfer in all $l=2$ cases except for 3^+ states where only $d_{5/2}$ transfer is allowed. Hence the quoted numbers are only a lower bound on the possible $d_{5/2}$ strength. Nonetheless, the fragmentary evidence cited in Sec. VI does suggest that the model over predicts $d_{5/2}$ core excitation.

B. Odd-parity states

Only the single-particle shell-model estimates exist for the odd-parity levels. However, the conclusions from the analysis of the even-parity levels are used to present in Table VII the experimental summed strengths of the $l=1$ and $l=3$ transitions: Whether, as the experimental sums are multiplied by 0.75 or not, they amount to 50% or 75%, respectively, of the shell-model limit for $l=1$ as well as for $l=3$ transitions (with the restriction of transitions only to the $f_{7/2}$ and $p_{3/2}$ orbits). Some weakly populated odd-parity levels can have escaped observation because they are unresolved from more strongly populated levels. For instance, from the (p,γ) and (p,p) reactions on ^{31}P (Ref. 3) two levels are known to lie at $E_x=10287$ and 10289 keV, ($J^\pi=3^-$, $l=3$, $T=0+1$) and ($J^\pi=2^-$, $l=1$, $T=0+1$), respectively. In the present work only the $l=3$ transition was observed with a spectroscopic strength of 0.26. The spectroscopic strength of the $l=1$ transition to the $E_x=10289$ keV level can be estimated as 0.011 from the proton partial width ($\Gamma_p=125\pm20$ eV, Ref. 3) and from the single-particle width, $\Gamma_{s.p.}=27.4$ keV, obtained from the GAMOV code (see Sec. IV). Such a transition is too weak to produce an observable change in the shape of the dominant $l=3$ transition to the $E_x=10287$ keV level.

It must also be pointed out that the spectroscopic strengths collected in Fig. 7 and Table VII are from 61 levels only out of the 111 which were observed in the present work. So the missing $l=1$ and $l=3$ strength can be also spread partly over the many levels observed between 11.2 and 12.5 MeV for which no l assignment could be made, and partly over higher-lying states.

ACKNOWLEDGMENTS

The authors are grateful to Dr. S. Galès for his help during the DWBA analysis of the angular distributions leading to unbound states. They are also indebted to D. Snajzderman for the phosphorus target preparation. They acknowledge the operating crew of the Orsay tandem Van de Graaff for the efficient running of the accelerator.

*John Simon Guggenheim Memorial Foundation Fellow, 1977.
†Research supported in part by the U. S. National Science Foundation.

[1]A. Graue, L. Herland, J. R. Lien, and E. R. Cosman, Nucl. Phys. A210, 513 (1968).
[2]J. B. French and M. H. MacFarlane, Nucl. Phys. 26, 168 (1961).
[3]J. Vernotte, S. Galès, M. Langevin, and J. M. Maison, Nucl. Phys. A212, 493 (1973).
[4]J. J. M. Van Gasteren, A. J. L. Verhage, and J. F. Van Der Veen, Nucl. Phys. A210, 29 (1973).
[5]J. Uzureau, A. Adam, O. Bersillon, and S. Joly, Nucl. Phys. A267, 217 (1976).
[6]D. L. Show, A. S. Moalem, and B. H. Wildenthal, Bull. Am. Phys. Soc. 19, 74 (1974).
[7]H. Nann and B. H. Wildenthal, Phys. Rev. C 13, 1009 (1976).
[8]B. W. Hooton, Nucl. Instrum. Methods 27, 338 (1964).
[9]J. R. Comfort, Argonne National Laboratory Physics Division Informal Report No. Phy-1970 B (unpublished).
[10]J. Vernotte, S. Galès, M. Langevin, and J. M. Maison, Phys. Rev. C 8, 178 (1973).
[11]P. M. Endt and C. van Der Leun, Nucl. Phys. A214, 1 (1973).
[12]R. H. Bassel, Phys. Rev. 149, 791 (1966).
[13]T. Tamura, W. R. Coker, and F. J. Rybicki, Comp. Phys. Comm. 2, 94 (1971).
[14]F. Perey, private communication.
[15]W. W. Dykoski and D. Dehnard, Phys. Rev. C 13, 80 (1976).
[16]J. Kalifa, G. Rotbard, M. Vergnes, and G. Ronsin, J. Phys. (Paris) 34, 139 (1973).
[17]E. Newman, L. C. Becker, B. M. Preedom, and J. C. Hiebert, Nucl. Phys. A100, 236 (1967).
[18]W. R. Coker and G. W. Hoffmann, Z. Phys. 263, 179 (1973).
[19]W. R. Coker, Phys. Rev. C 7, 2426 (1973).
[20]J. Vernotte, J. M. Maison, A. Chevallier, A. Huck, C. Miehe, and G. Walter, Phys. Rev. C 13, 984 (1976).
[21]D. W. O. Rogers, W. R. Dixon, and R. S. Storey, Nucl. Phys. A281, 345 (1977).
[22]P. R. Gardner, D. C. Kean, R. H. Spear, A. M. Baxter, R. A. I. Bell, and L. E. Carlson, Aust. J. Phys. 26, 747 (1973).
[23]J. Källne and O. Sundberg, Phys. Scr. 4, 243 (1971).
[24]J. Uzureau, A. Adam, O. Bersillon, and S. Joly, Nucl. Phys. A267, 245 (1976).
[25]J. Vernotte (unpublished).
[26]R. A. Lindgren, J. P. Trentelman, N. Anantaraman, H. E. Gove, and F. C. Jundt, Phys. Lett. 49B, 263 (1974).
[27]I. Forsblom, P. Paukku, and S. Penttinen, Comment. Phys.-Math. 40, 1 (1970).
[28]G. A. Hokken, J. A. J. Hermans, and A. Van Ginkel, Nucl. Phys. A211, 405 (1973).
[29]F. E. H. Van Eijkern, G. Van Middelkoop, J. Timmer, and J. A. Van Luijk, Nucl. Phys. A210, 38 (1973).
[30]F. E. H. Van Eijkern, G. Van Middelkoop, W. A. Sterrenburg, and A. F. C. Buijense, Nucl. Phys. A260, 124 (1976).
[31]W. Chung and B. H. Wildenthal (unpublished).